Transfection, immunoprecipitation and western blotting

Human embryonic kidney (HEK) 293T and COS7 cells were maintained in Dulbecco's modified Eagle's medium (DMEM) supplemented with 10% fetal calf serum. Cells were co-transfected with 3 μg of each plasmid and cultured for 48 h. For *in vivo* stimulation experiments, cells were grown for 48 h in spent medium and then stimulated with HGF (400 U ml^{-1}) at 37 °C, for the indicated times. Ubiquitination experiments were performed as described[15].

For immunoprecipitations, cells were lysed with EB buffer (20 mM Tris-HCl, pH 7.4, 5 mM EDTA, 150 mM NaCl, 10% glycerol, 1% Triton X-100) in the presence of protease inhibitors and 1 mM Na-orthovanadate. After immunoprecipitation with the appropriate antibodies, high stringency washes were performed (EB plus 1 M LiCl).

Western blots were performed according to standard methods. In western blot and immunoprecipitations the following antibodies were used: PY20 monoclonal antibody (Transduction Laboratories), anti-Met antibodies (described in ref. 25), anti vesicular stomatitis virus (VSV)-G (Sigma), anti-Cbl and anti-haemagglutinin (HA) (Santa Cruz Biotechnology), anti-Gab1 (Upstate Biotechnology), and anti-Flag (Sigma). Monoclonal anti-endophilin A3 and polyclonal anti-endophilins antibodies (able to recognize endophilins A1, A2 and A3) were a gift of E. Lantelme and C. Giachino. Anti-CIN85 (CT) antibody and pre-immune serum were provided by I. Dikic. Final detection was done with ECL system (Amersham).

GST pull-down assay

The host strain *Escherichia coli* XL-1 was transformed with plasmids encoding GST fusion proteins, and protein expression was induced with isopropyl-β-D-thiogalactopyranoside. Bacterial cells were lysed in phosphate-buffered saline containing 1% Triton X-100 and protease inhibitors. Fusion proteins were captured on glutathione–Sepharose beads and incubated with crude lysates of transfected HEK 293T cells at 4 °C for 2 h. The beads were washed extensively in lysis buffer, and then bound proteins were eluted by boiling in SDS–polyacrylamide gel electrophoresis (PAGE) sample buffer, separated by SDS–PAGE, and processed for western blotting.

Motility assay

For motility assay, 10^5 cells were seeded on the upper side of a Transwell chamber on a porous polycarbonate membrane (8.0-μm pore size); the lower chamber of the Transwell was filled with DMEM containing 5% FBS, either in the absence or in the presence of HGF (100 or 200 U ml^{-1}). After 24 h of incubation, cells attached to the upper side of the filter were mechanically removed. Cells that migrated to the lower side were fixed and stained with crystal violet. The stained cells were solubilized in 10% acetic acid, absorbance at 560 nm was measured in a micro-plate reader.

Immunofluorescence

COS7 cells were transfected using Lipofectamine (Life Technologies) and then seeded on polylisine-coated coverslips. Cells were treated with HGF (400 U ml^{-1}) for different times, then fixed in 4% paraformaldehyde, permeabilized in 0.1% Triton X-100 and finally co-stained using biotin-conjugated anti-HGF (R&D), anti-VSV to detect endophilin A3 SH3 domain, anti-Flag to detect CIN85-PCC, and anti-HA to detect Cbl-480. Images were taken using a Bio-Rad Confocal Microscopy System.

Received 12 November 2001; accepted 7 January 2002.

1. Jeffers, M., Taylor, G. A., Weidner, K. M., Omura, S. & Vande Woude, G. F. Degradation of the Met tyrosine kinase receptor by the ubiquitin-proteasome pathway. *Mol. Cell. Biol.* **17,** 799–808 (1997).
2. Hammond, D. E., Urbé, S., Vande Woude, G. F. & Clague, M. J. Down-regulation of MET, the receptor for hepatocyte growth factor. *Oncogene* **20,** 2761–2770 (2001).
3. Giachino, C. *et al.* A novel SH-3-containing human gene family preferentially expressed in the central nervous system. *Genomics* **41,** 427–434 (1997).
4. Schmidt, A. *et al.* Endophilin I mediates synaptic vesicle formation by transfer of arachidonate to lysophosphatidic acid. *Nature* **401,** 133–141 (1999).
5. Take, H. *et al.* Cloning and characterization of a novel adaptor protein, CIN85, that interacts with c-Cbl. *Biochem. Biophys. Res. Commun.* **268,** 321–328 (2000).
6. Hunter, T. Signaling—2000 and beyond. *Cell* **100,** 113–127 (2000).
7. Waterman, H. & Yarden, Y. Molecular mechanisms underlying endocytosis and sorting of ErbB receptor tyrosine kinases. *FEBS Lett.* **490,** 142–152 (2001).
8. Di Fiore, P. P. & De Camilli, P. Endocytosis and signaling: an inseparable partnership. *Cell* **106,** 1–4 (2001).
9. Ringstad, N., Nemoto, Y. & De Camilli, P. The SH3p4/SH3p8/SH3p13 protein family: binding partners for synaptojanin and dynamin via a Grb2-like Src homology 3 domain. *Proc. Natl Acad. Sci. USA* **94,** 8569–8574 (1997).
10. Kirsch, K. H., Georgescu, M. M., Ishimura, S. & Hanafusa, H. CMS: an adapter molecule involved in cytoskeletal rearrangements. *Proc. Natl Acad. Sci. USA* **99,** 6211–6216 (1999).
11. Dustin, M. L. *et al.* A novel adaptor protein orchestrates receptor patterning and cytoskeletal polarity in T-cell contacts. *Cell* **94,** 667–677 (1998).
12. Cestra, G. *et al.* The SH3 domains of Endophilin and Amphiphysin bind to the proline rich region of Synaptojanin 1 at distinct sites that display an unconventional binding specificity. *J. Biol. Chem.* **274,** 32001–32007 (1999).
13. Watanabe, S. *et al.* Characterization of the CIN85 adaptor protein and identification of components involved in CIN85 complexes. *Biochem. Biophys. Res. Commun.* **278,** 167–174 (2000).
14. Thien, C. B. F. & Langdon, W. Y. Cbl: many adaptations to regulate protein tyrosine kinases. *Nature Rev. Mol. Cell Biol.* **2,** 294–307 (2001).
15. Levkowitz, G. *et al.* Ubiquitin ligase activity and tyrosine phosphorylation underlie suppression of growth factor signaling by c-Cbl/Sli-1. *Mol. Cell* **4,** 1029–1040 (1999).
16. Fixman, E. D. *et al.* Efficient cellular transformation by the Met oncoprotein requires a functional Grb2 binding site and correlates with phosphorylation of the Grb2-associated proteins, Cbl and Gab1. *J. Biol. Chem.* **272,** 20167–20172 (1997).
17. Giordano, S., Ponzetto, C., Di Renzo, M. F., Cooper, C. S. & Comoglio, P. M. Tyrosine kinase receptor indistinguishable from the c-met protein. *Nature* **339,** 155–156 (1989).
18. Weidner, K. M. *et al.* Interaction between Gab1 and the c-Met receptor tyrosine kinase is responsible for epithelial morphogenesis. *Nature* **384,** 173–176 (1996).
19. Ponzetto, C. *et al.* A multifunctional docking site mediates signaling and transformation by the hepatocyte growth factor/scatter factor receptor family. *Cell* **77,** 261–271 (1994).
20. Garcia-Guzman, M., Larse, E. & Vuori, K. The proto-oncogene c-Cbl is a positive regulator of Met-induced MAP kinase activation: a role for the adaptor protein Crk. *Oncogene* **19,** 4058–4065 (2000).
21. Brodin, L., Low, P. & Shupliakov, O. Sequential steps in clathrin-mediated synaptic vesicle endocytosis. *Curr. Opin. Neurobiol.* **10,** 312–320 (2000).
22. Huttner, W. B. & Schmidt, A. Lipids, lipid modification and lipid-protein interaction in membrane budding and fission-insights from the roles of endophilin A1 and synaptophysin in synaptic vesicle endocytosis. *Curr. Opin. Neurobiol.* **10,** 543–551 (2000).
23. Hill, E., van Der Kaay, J., Downes, C. P. & Smythe, E. The role of dynamin and its binding partners in coated pit invagination and scission. *J. Cell Biol.* **152,** 309–323 (2001).
24. Soubeyran, P., Kowanetz, K., Szymkiewicz, I., Langdon, W. Y. & Dikic, I. Cbl–CIN85–endophilin complex mediates ligand-induced downregulation of EGF receptors. *Nature* **416,** 183–187 (2001).
25. Prat, M., Crepaldi, T., Pennacchietti, S., Bussolino, F. & Comoglio, P. M. Agonistic monoclonal antibodies against the Met receptor dissect the biological responses to HGF. *J. Cell Sci.* **111,** 237–247 (1998).

Supplementary Information accompanies the paper on *Nature*'s website (http://www.nature.com).

Acknowledgements

We thank E. Lantelme, C. Giachino and L. Lanzetti for production of anti-endophilin antibodies and for GST–Endo3, GST–Endo1-2-SH3 constructs; L. Tamagnone for ΔPlexin A3 cDNA; P. De Camilli for dynamin cDNA; Y. Yarden for Cbl and ubiquitin plasmids; I. Dikic for CIN85 reagents and Cbl-ΔSH2 plasmid; and W. Y. Langdon for Cbl-70Z and Cbl-480 constructs. We also thank Y. Yarden, L. Tamagnone and our colleagues for discussions; A. Cignetto for secretarial assistance; and E. Wright for editing the manuscript. The technical assistance of L. Palmas, R. Albano and E. Clemente is acknowledged. This work was partly supported by Associazione E. & E. Rulfo per la Genetica Medica to N.M., by Italian Association for Cancer Research to P.M.C. and by MURST COFIN to S.G.

Competing interests statement

The authors declare that they have no competing financial interests.

Correspondence and requests for materials should be addressed to S.G. (e-mail: sgiordano@ircc.unito.it).

Involvement of receptor-interacting protein 2 in innate and adaptive immune responses

Arnold I. Chin*†, Paul W. Dempsey†‡, Kevin Bruhn‡, Jeff F. Miller*‡, Yang Xu§ & Genhong Cheng*‡

** Molecular Biology Institute, University of California, Los Angeles, California 90095, USA*
‡ Department of Microbiology, Immunology, and Molecular Genetics, Jonsson Comprehensive Cancer Center, University of California, Los Angeles, California 90095, USA
§ Section of Molecular Biology, Division of Biology, University of California, San Diego, California 92093, USA
† These authors contributed equally to this work

Host defences to microorganisms rely on a coordinated interplay between the innate and adaptive responses of immunity[1]. Infection with intracellular bacteria triggers an immediate innate response requiring macrophages, neutrophils and natural killer cells, whereas subsequent activation of an adaptive response through development of T-helper subtype 1 cells (T_H1) proceeds during persistent infection[1]. To understand the physiological

© 2002 Macmillan Magazines Ltd

role of receptor-interacting protein 2 (Rip2), also known as RICK and CARDIAK, we generated mice with a targeted disruption of the gene coding for Rip2. Here we show that Rip2-deficient mice exhibit a profoundly decreased ability to defend against infection by the intracellular pathogen *Listeria monocytogenes*. Rip2-deficient macrophages infected with *L. monocytogenes* or treated with lipopolysaccharide (LPS) have decreased activation of NF-κB, whereas dominant negative Rip2 inhibited NF-κB activation mediated by Toll-like receptor 4 and Nod1. *In vivo*, Rip2-deficient mice were resistant to the lethal effects of LPS-induced endotoxic shock. Furthermore, Rip2 deficiency results in impaired interferon-γ production in both T_H1 and natural killer cells, attributed in part to defective interleukin-12-induced Stat4 activation. Our data reflect requirements for Rip2 in multiple pathways regulating immune and inflammatory responses.

Rip2 contains an amino-terminal kinase domain and a carboxy-terminal caspase activation and recruitment domain (CARD)[2–4]. We disrupted the *Rip2* gene in mice by replacing the first exon of Rip2 with a neomycin-resistance gene (Fig. 1a). Targeted disruption was determined by Southern analysis (Fig. 1b), and loss of Rip2 expression was demonstrated by western analysis (Fig. 1c). $Rip2^{-/-}$ mice were viable and fertile, and have survived up to 24 months with no gross differences compared to $Rip2^{+/+}$ littermates. Offspring genotypes from heterozygous breeding approached mendelian frequency. Development and ratios of all haematopoietic lineages tested appeared equivalent in $Rip2^{+/+}$ and $Rip2^{-/-}$ mice by analysis of typical surface markers. Overexpressed Rip2 has been shown to promote apoptosis[2,3]; however, sensitivity to apoptosis induced by a variety of stimuli was similar in $Rip2^{+/+}$ and $Rip2^{-/-}$ embryonic fibroblast cells and thymocytes (data not shown).

As Rip2 interacts with CD40, a co-stimulatory receptor critical for T-cell-dependent humoral responses[2], we assessed the role of Rip2 in the humoral immune response. On immunization of mice with the T-cell-dependent antigen chicken egg ovalbumin (OVA), we observed that titres of OVA-specific immunoglobulin-γ (IgG)-2a were up to 20-fold lower in $Rip2^{-/-}$ mice compared with $Rip2^{+/+}$ mice (Fig. 2a). In contrast, OVA-specific IgG1 titres were similar in $Rip2^{+/+}$ and $Rip2^{-/-}$ mice (Fig. 2b). No significant differences in B-cell proliferation were found between $Rip2^{+/+}$ and $Rip2^{-/-}$ B cells stimulated with anti-CD40 and anti-IgM (Fig. 2c, d). On the other hand, decreased proliferation was observed in $Rip2^{-/-}$ $CD4^+$ T cells stimulated with anti-CD3 compared with $Rip2^{+/+}$ $CD4^+$ T cells (Fig. 2e). As a role for Rip2 in T cells was unexpected, we also examined *Rip2* gene expression, and detected increasing levels of Rip2 messenger RNA during activation of T cells (Fig. 2f).

To explore the ability of Rip2 to regulate T-cell responses, we immunized $Rip2^{+/+}$ and $Rip2^{-/-}$ mice with OVA in complete Freund's adjuvant (CFA)[5]. Consistent with the decreased immunoglobulin isotype switching to IgG2a, lower amounts of IFN-γ were produced by $Rip2^{-/-}$ draining lymph node cells restimulated with antigen (Fig. 3a; see also ref. 6). These data suggest impaired T_H1 activation in $Rip2^{-/-}$ mice, a function critical for the generation of cell-mediated and inflammatory responses to pathogen challenge[7,8]. To further investigate T-helper cell development, we cultured $Rip2^{+/+}$ and $Rip2^{-/-}$ $CD4^+$ T cells under polarizing conditions to promote either T_H1 or T_H2 development. When restimulated with anti-CD3, T_H1 cells of $Rip2^{-/-}$ mice produced twofold less IFN-γ than T_H1 cells of $Rip2^{+/+}$ mice (Fig. 3b). In contrast, similar levels of interleukin (IL)-4 were secreted in $Rip2^{-/-}$ and $Rip2^{+/+}$ T_H2-polarized cells, suggesting that $Rip2^{-/-}$ T cells have an impaired ability to differentiate into T_H1 cells, but a normal capacity to differentiate into T_H2 cells (Fig. 3c).

To specifically study T_H1 cells, we generated T_H1 clones. In $CD4^+$ T cells, IFN-γ production can be induced either through T-cell

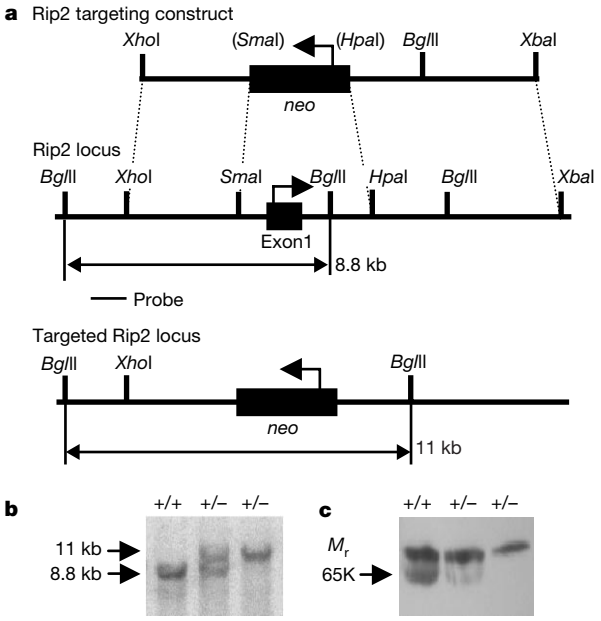

Figure 1 Generation of Rip2-deficient mice. **a**, Schematic representation of the gene-targeting construct (top), the genomic Rip2 locus (middle), and the targeted Rip2 locus (bottom). The probe for Southern analysis is indicated. **b**, Genomic tail DNA was digested with *Bgl*II, and blots were hybridized with the probe indicated in **a**. **c**, Extracts from splenocytes of $Rip2^{+/+}$, $Rip2^{+/-}$, and $Rip2^{-/-}$ mice were examined by western analysis using a Rip2-specific antibody. M_r, relative molecular mass.

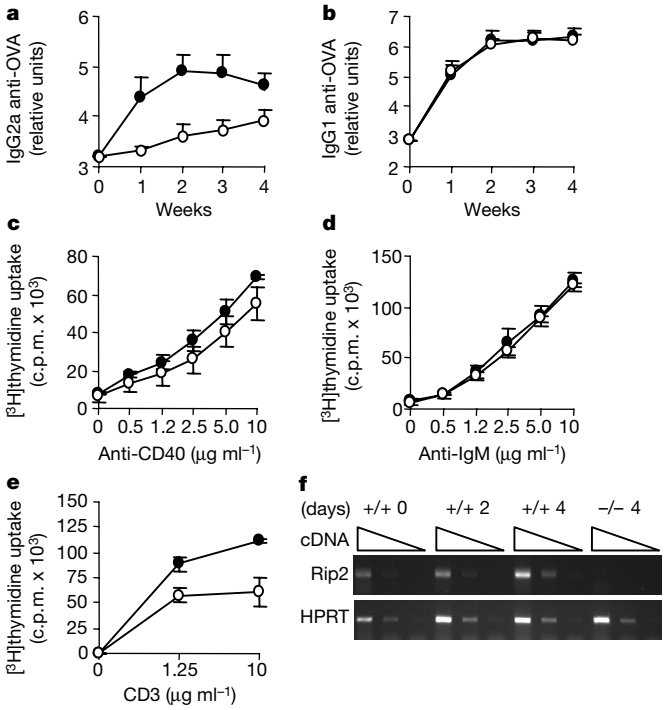

Figure 2 Impaired isotype switching and T-cell proliferation in $Rip2^{-/-}$ cells. **a**, **b**, Sera from $Rip2^{+/+}$ (filled circles) and $Rip2^{-/-}$ (open circles) mice immunized with OVA (100 μg) adsorbed on alum were used to measure levels of IgG2a (**a**) or IgG1 (**b**) using isotype-specific antibodies by ELISA. *y* axis is on a logarithmic scale. **c**, **d**, Purified $Rip2^{+/+}$ (filled circles) or $Rip2^{-/-}$ (open circles) splenic B cells were stimulated with anti-CD40 (**c**) or anti-IgM (**d**) for 48 h, and assessed for proliferation. **e**, Purified $Rip2^{+/+}$ (filled circles) and $Rip2^{-/-}$ (open circles) $CD4^+$ T cells were stimulated with anti-CD3 for 48 h. Proliferation was assessed by addition of [^{3}H]thymidine. **f**, Serial dilutions of template cDNA (1:1, 1:10, 1:100) were used for semi-quantitative RT–PCR measuring Rip2 expression during T-cell differentiation after 0, 2, and 4 days for $Rip2^{+/+}$, and 4 days for $Rip2^{-/-}$ $CD4^+$ T cells.

© 2002 Macmillan Magazines Ltd

antigen receptor (TCR) or IL-12/IL-18 activation[9]. To delineate the specific pathway involving Rip2 in IFN-γ regulation, we stimulated T_H1 clones with IL-12, IL-18, or both, and measured IFN-γ production. Whereas IL-12 or IL-18 alone did not activate IFN-γ secretion, *Rip2*$^{-/-}$ T_H1 clones produced 76% less IFN-γ on average after synergistic activation with the combination of IL-12 and IL-18, compared with *Rip2*$^{+/+}$ clones. After stimulation with anti-CD3 alone, or with IL-12, IL-18, or IL-12 plus IL-18, in conjunction with TCR activation, *Rip2*$^{-/-}$ clones produced 34%, 43%, 45% or 36% less IFN-γ on average, respectively, than *Rip2*$^{+/+}$ cells (Fig. 3d). Statistically significant differences in IL-12-mediated IFN-γ production led us to examine further the role of Rip2 in IL-12 signalling.

IL-12 mediates its function largely through the activation of signal transducer and activator of transcription 4 (Stat4). Indeed, *Stat4*$^{-/-}$ T_H1 cells are defective in IL-12-induced IFN-γ production[10,11]. Similar expression levels of IL-12 receptor in *Rip2*$^{+/+}$ and *Rip2*$^{-/-}$ clones, as measured by western blot and polymerase chain reaction with reverse transcription (RT-PCR) (data not shown), implicated Rip2 as functioning downstream of the IL-12 receptor. To determine whether the loss of Rip2 affected Stat4 activation, we stimulated *Rip2*$^{+/+}$ and *Rip2*$^{-/-}$ T_H1 clones with IL-12, and measured activation of Stat4. *Rip2*$^{-/-}$ T_H1 clones exhibited impaired Stat4 activation, as shown by decreased tyrosine phosphorylation and decreased DNA binding, whereas total amounts of Stat4 remained constant (Fig. 3e). Thus, defective Stat4 activation may contribute towards impaired IFN-γ production in *Rip2*$^{-/-}$ mice.

The inflammatory cytokine IL-12 bridges innate and adaptive immunity, in part, by induction of IFN-γ, a critical mediator of T_H1, cytotoxic T-lymphocyte (CTL), and natural killer (NK) cell responses[12]. We next investigated whether impaired IL-12-mediated IFN-γ production in T_H1 cells of *Rip2*$^{-/-}$ mice could be a generalized defect, and examined the ability of NK cells to respond to IL-12. Splenocytes from *Rip2*$^{+/+}$ and *Rip2*$^{-/-}$ mice were stimulated with IL-12, IL-18, or both IL-12 and IL-18. Whereas splenocytes of *Rip2*$^{+/+}$ mice secreted IFN-γ after stimulation with IL-12 or IL-18, splenocytes of *Rip2*$^{-/-}$ mice did not secrete IFN-γ at levels above background under similar conditions, demonstrating an impairment of IL-12 and IL-18 signalling in NK cells. Synergistic activation with IL-12 and IL-18 induced twofold less IFN-γ from *Rip2*$^{-/-}$ cells (Fig. 3f). Impairments in IL-18-mediated signalling were observed in both T_H1 and NK cells. This finding indicates an additional role for Rip2 in the related Toll-like receptor (TLR)/IL-1/IL-18 superfamily.

IFN-γ is crucial in the defence against intracellular pathogens such as *L. monocytogenes*, as mice deficient in IFN-γ, IFN-γR, or Stat4 have increased susceptibility to infection by *L. monocytogenes*[11,13,14]. To demonstrate the *in vivo* role of Rip2 in immune responses, we used a 10% LD_{50} dose (lethal to 50% of animals tested) of *L. monocytogenes* to intravenously infect *Rip2*$^{+/+}$ and *Rip2*$^{-/-}$ mice. Although the bacterial titres among *Rip2*$^{+/+}$ and *Rip2*$^{-/-}$ mice after 1.5 days were similar in both livers and spleens, after 5 days the numbers of *L. monocytogenes* recovered from the livers and spleens of *Rip2*$^{-/-}$ mice were about 75- and 25-fold higher than those in *Rip2*$^{+/+}$ mice, respectively (Fig. 4a, b). Indeed, all *Rip2*$^{-/-}$ mice succumbed to infection within 8 days, whereas 83% of *Rip2*$^{+/+}$ mice survived and completely cleared the bacteria by 10 days (Fig. 4c).

Interestingly, up to tenfold higher *L. monocytogenes* titres were found in *Rip2*$^{-/-}$ mice 3 days after infection, earlier than the 4–5 days required for the development of an adequate adaptive response, suggesting an intrinsic defect in innate immunity as well. Thus, to examine the intrinsic contribution of Rip2 in macrophages, we investigated signalling in macrophages infected

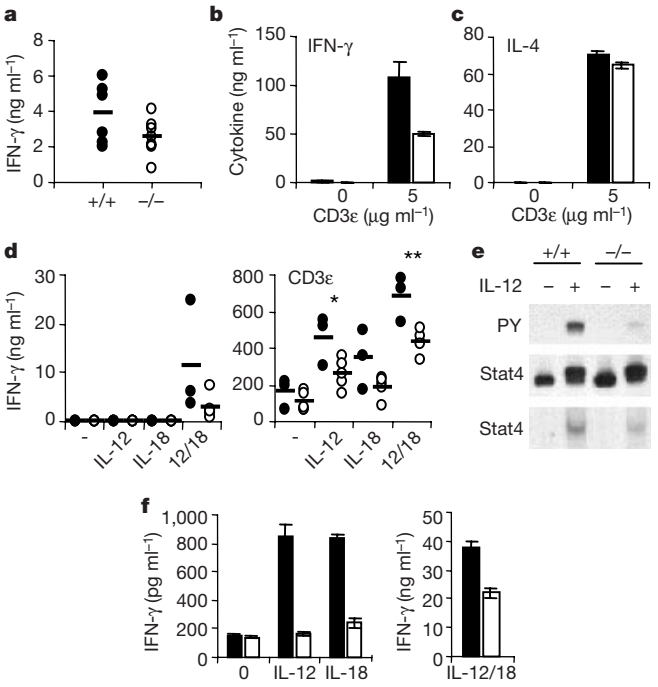

Figure 3 Impaired IL-12- and IL-18-induced activation of T_H1 and NK cells in *Rip2*$^{-/-}$ mice. **a**, Lymph node cells from OVA (100 μg) in CFA-immunized *Rip2*$^{+/+}$ (filled circles) and *Rip2*$^{-/-}$ (open circles) mice were cultured with OVA for 24 h before measuring IFN-γ production by ELISA. The horizontal bar indicates mean IFN-γ levels. **b**, **c**, Splenic $CD4^+$ T cells of *Rip2*$^{+/+}$ (filled circles) and *Rip2*$^{-/-}$ (open circles) mice were cultured with anti-CD3 under T_H1-polarizing conditions (**b**) or under T_H2-polarizing conditions (**c**). Differentiated cells were restimulated with anti-CD3, and levels of cytokines were measured. **d**, T_H1 clones of *Rip2*$^{+/+}$ (filled circles) and *Rip2*$^{-/-}$ (open circles) mice were cultured with anti-CD3 as indicated, and assayed for IFN-γ production. Asterisk, $P < 0.04$ compared with *Rip2*$^{+/+}$ cells; double asterisk, $P < 0.01$ compared with *Rip2*$^{+/+}$ cells. **e**, T_H1 clones of *Rip2*$^{+/+}$ and *Rip2*$^{-/-}$ mice were stimulated with IL-12 as indicated. Immunoprecipitated Stat4 proteins were analysed by western analysis for phosphotyrosine (top circles), and for total Stat4 levels (middle circles). Activation of Stat4 was detected by EMSA (bottom). **f**, Splenocytes of *Rip2*$^{+/+}$ (filled circles) and *Rip2*$^{-/-}$ (open circles) mice were stimulated as indicated, then evaluated for IFN-γ production.

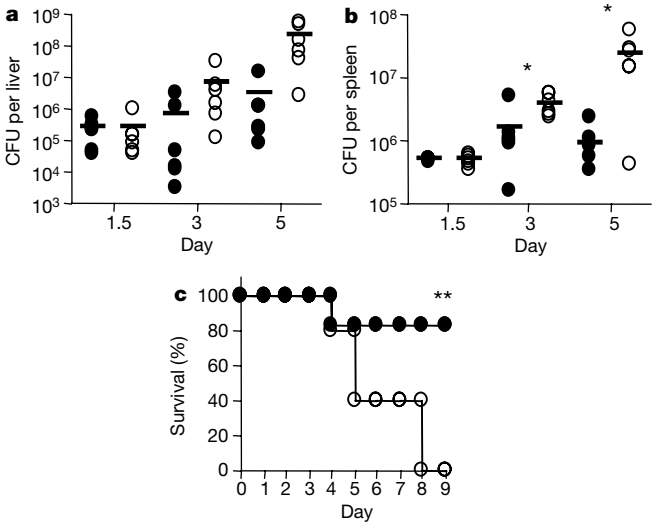

Figure 4 Increased susceptibility to *Listeria monocytogenes* in *Rip2*$^{-/-}$ mice. **a**–**c**, *Rip2*$^{+/+}$ (filled circles) and *Rip2*$^{-/-}$ (open circles) mice were infected intravenously with 3×10^3 colony-forming units (CFU) of *L. monocytogenes*. 1.5, 3, or 5 days after infection, livers (**a**) and spleens (**b**) were collected and bacterial titres determined. Survival was determined after 9 days (**c**). Horizontal bars represent means. Asterisk, $P < 0.05$ compared with *Rip2*$^{+/+}$ mice; double asterisk, $P < 0.01$ compared with *Rip2*$^{+/+}$ mice.

© 2002 Macmillan Magazines Ltd

with *L. monocytogenes*. Decreased activation of NF-κB (Fig. 5a), a pathway critical to host inflammatory responses, was observed in macrophages of *Rip2*$^{-/-}$ mice. Similar to infection with *L. monocytogenes*, LPS-stimulated macrophages of *Rip2*$^{-/-}$ mice showed decreased activation of NF-κB compared with *Rip2*$^{+/+}$ cells (Fig. 5b), as well as decreased p38 and SAPK activation (data not shown). In addition, LPS stimulation upregulated Rip2 expression as measured by RT-PCR (data not shown). To assess *in vivo* responsiveness, we challenged *Rip2*$^{+/+}$ and *Rip2*$^{-/-}$ mice with LPS, and found that *Rip2*$^{-/-}$ mice were completely resistant to an LD_{50} dose (Fig. 5c). This effect underscores the importance of Rip2 in the recognition and/or subsequent activation of inflammatory responses to LPS, and highlights a common signalling defect in *Rip2*$^{-/-}$ mice in TLR and related receptors such as IL-18.

Recent studies have implicated the plant disease-resistance-like proteins, Nod1 and Nod2, as activators of NF-κB in response to presentation of pathogens in the cytosol[15]. In fact, mutations in Nod2 have been linked to susceptibility to Crohn's disease, implicating innate immune dysfunction in Crohn's disease[16,17]. Considering how Rip2-deficient mice could respond *in vivo* with altered sensitivity to both LPS and *L. monocytogenes*, we investigated a role for Rip2 in the signalling pathway of TLRs and Nods. Activation of NF-κB by both TLR4 and Nod1 was inhibited in a dose-dependent manner by coexpression of dominant negative Rip2 (Rip2-DN), as measured by a NF-κB-dependent luciferase reporter in 293T cells (Fig. 5d). Whereas activation of NF-κB by both TLR4 and Nod1 was inhibited using a dominant active inhibitor of NF-κB (IκB-DA), dominant negative forms of proteins found in TLR complexes (IRAK-DN and MyD88-DN) specifically abolished TLR4- but not Nod1-induced NF-κB activity. These data are consistent with previous studies demonstrating association of Rip2 with either Nod1 or TRAF6, and further supports a Rip2-dependent contribution in TLR/IL-18 receptor and Nod1 family signalling[18–20].

Insight into the regulation of cell-mediated immunity is critical to understanding the balance between normal immune responses and inappropriate inflammatory responses. Our studies provide genetic evidence for the requirement of Rip2 in both innate and adaptive immune responses. In the future, it will be important to establish the precise mechanisms of Rip2 function in IL-12/Stat4 signalling, as well as in *in vivo* specificity in intracellular versus extracellular microbial infections. Here, we implicate Rip2 in the innate response to pathogens by mediating Nod- and TLR-induced cell signalling. In the adaptive immune response, Rip2 mediates cytokine-induced IFN-γ production in T_H1 and NK cells. The critical roles of Rip2 in regulating cell-mediated responses provide support for Rip2 as a candidate target for immune intervention. □

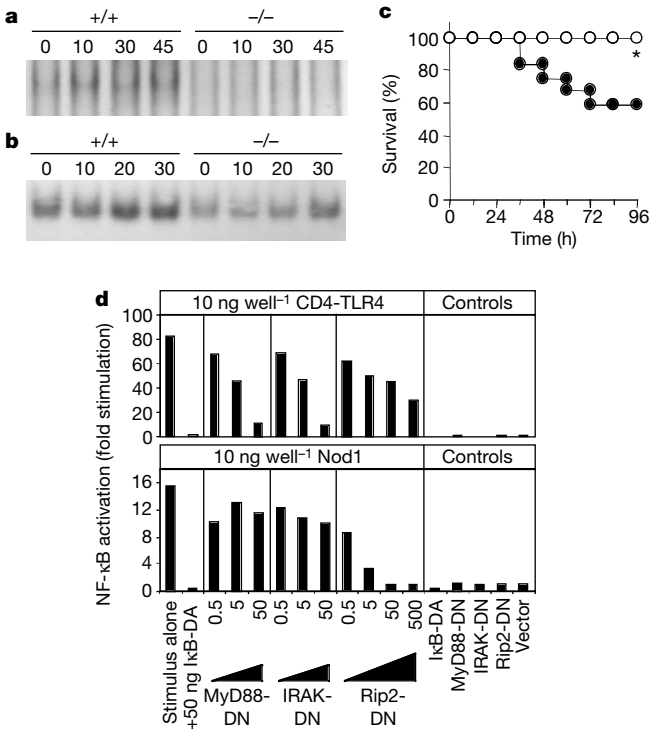

Figure 5 Impaired NF-κB activation in macrophages of *Rip2*$^{-/-}$ mice. **a**, **b**, Macrophages of *Rip2*$^{+/+}$ and *Rip2*$^{-/-}$ mice were stimulated with *L. monocytogenes* (**a**). IFNγ-activated macrophages of *Rip2*$^{+/+}$ and *Rip2*$^{-/-}$ mice were stimulated with LPS (**b**). Activation of NF-κB was determined by EMSA. **c**, Eleven *Rip2*$^{+/+}$ (filled circles) and twelve *Rip2*$^{-/-}$ (open circles) mice were intraperitoneally injected with 28 mg kg^{-1} body weight of LPS from *Escherichia coli* serotype O55:B5, and monitored for survival. Asterisk, $P < 0.001$ compared with *Rip2*$^{+/+}$ mice. **d**, Cell lysates from 293T cells transfected with the indicated constructs were analysed for luciferase activity of a NF-κB reporter. Normalized fold activation is indicated.

Methods

Generation of *Rip2*$^{-/-}$ mice

An internal 1.1-kilobase (kb) *Hpa*I–*Sma*I genomic fragment containing exon 1 was replaced with a PGK-*neo*^{r} (neomycin-resistance gene) cassette. The targeting construct was electroporated into 129J1 cells and selected with G418. Recombinants were identified using a genomic probe external to the targeting construct, hybridizing to an 8.8-kb *Bgl*II fragment of the endogenous Rip2 locus and to an 11-kb fragment of the targeted allele. We used Rip2-specific C-terminal antibodies for western analysis (Alexis Biochemicals). Two clones chosen for injection into 3.5-day-old C57Bl6 blastocytes gave germ-line transmission of the targeted allele. Chimaeric mice were crossed with C57Bl6 females to generate *Rip2*$^{+/-}$ mice. Mice were re-derived into a specific pathogen-free facility. Age- and gender-matched mice of C57Bl/6x129 F_2 background were used, except for *L. monocytogenes* infections, in which mice of C57Bl/6x129 F_5 generation were used.

PCR with reverse transcription

First strand complementary DNA was produced by reverse transcription (RT) of 5 μg total RNA using the superscript first strand synthesis kit (Gibco BRL). Levels of hypoxanthine guanine phosphoribosyltransferase (HPRT) were amplified by PCR and used to equalize levels of cDNA[21]. T cells were differentiated *in vitro* by stimulation with anti-CD3 (5 μg ml^{-1}) and anti-CD28 (1 μg ml^{-1}) antibodies without antigen-presenting cells. The primers used for Rip2 PCR were: 5′-CCATCCCGTACCACAAGCTC-3′ and 5′-GCAGG ATGCGGAATCTCAAT-3′.

In vitro CD4$^+$ T-cell differentiation

Splenic CD4$^+$ T cells were purified by negative selection using a magnetic cell sorter (Stem Cell) to 90–95% purity as determined by staining with fluorescein isothiocyanate-conjugated anti-CD4 and flow cytometry. CD4$^+$ depleted splenocytes were used as APCs. Purified T cells (5×10^5 ml^{-1}) were cultured with wild-type irradiated APCs (5×10^5ml^{-1}) in the presence of anti-CD3 (5 μg ml^{-1}) and IL-2 (20 U ml^{-1}). T_H1 polarization was achieved with the addition of IL-12 (5 ng ml^{-1}) and anti-IL-4 (4 μg ml^{-1}), whereas for T_H2 polarization, IL-4 (1,000 U ml^{-1}) and anti-IFN-γ (4 μg ml^{-1}) was added. After 4 days of culture, cells were collected, washed extensively, and restimulated at 5×10^5 cells ml^{-1} with plate-bound anti-CD3 (5 μg ml^{-1}). Supernatants were collected after 24 h and assayed for levels of IFN-γ and IL-4 by ELISA. Antibodies for differentiation and ELISA assays were purchased from Pharmingen.

IFN-γ production in T_H1 clones and NK cells

T_H1 clones were maintained using irradiated wild-type APCs, and used for experiments 2 weeks after restimulation to decrease the contribution of cells from the APC population. T_H1 clones were cultured with media, IL-12 (1 ng ml^{-1}), IL-18 (50 ng ml^{-1}), or both, with and without plate-bound anti-CD3 (5 μg ml^{-1}) for 48 h. Splenocytes were stimulated with media, IL-12 (5 ng ml^{-1}), IL-18 (20 ng ml^{-1}), or both for 24 h. FACS analysis of splenocytes using a NK-specific antibody in conjunction with intracellular IFN-γ staining demonstrated that IFN-γ secreted from splenocytes was derived from NK cells, and that similar numbers of NK cells were present in spleens of *Rip2*$^{+/+}$ and *Rip2*$^{-/-}$ mice. Supernatants were assessed for IFN-γ production by ELISA.

Analysis of Stat4 activation

T_H1 clones from *Rip2*$^{+/+}$ and *Rip2*$^{-/-}$ mice were stimulated with IL-12 (10 ng ml^{-1}) for 15 min. We prepared total cell extracts as described[22]. Stat4 immunoprecipitated with polyclonal anti-Stat4 antibodies (Santa Cruz) was assessed for phosphotyrosine with RC-20-horseradish peroxidase (Transduction Laboratories). After stripping, total Stat4 levels were detected using rabbit anti-Stat4 antibody. For DNA binding, lysates (20 μg) were incubated with ^{32}P-labelled consensus binding site oligonucleotides for Stat4 (Santa Cruz), and analysed by electrophoresis mobility shift assay (EMSA).

NF-κB activation in macrophages

Total bone marrow cells were isolated from mice and plated overnight (1×10^6 cells ml^{-1}) in the presence of macrophage colony-stimulating factor (M-CSF). After 24 h,

© 2002 Macmillan Magazines Ltd

non-adherent cells were plated (1×10^5 ml^{-1}) and cultured for 6 days. Unactivated macrophages were stimulated with *L. monocytogenes* using a multiplicity of infection of 20, whereas macrophages activated with IFN-γ (400 U ml^{-1}) for 16 h were stimulated with LPS. Nuclear extracts (3 μg) were incubated with a ^{32}P-labelled oligonucleotide probe derived from the major histocompatibility complex (MHC) class II NF-κB consensus-binding site, and analysed by EMSA.

Transient transfection and luciferase analysis

Human embryonic kidney (293T) cells were plated in 6-well plates at 2.5×10^5 cells per well. Cells were stimulated by transfection with plasmid pCMV (cytomegalovirus) human NOD1 (10 ng) or pCMV murine CD4-TLR4 (10 ng). Stimulated cells were inhibited by co-transfection with pCMV human RIP2-DN (1–434), pcDNA3 murine MyD88-DN, pCiNeo murine IRAK-DN, or pCMV IκB-DA, as indicated (in ng). All transfections were performed with a luciferase reporter plasmid containing two κB binding sites (20 ng) and pCMV-LacZ (40 ng). Luciferase activity was measured and normalized to beta-galactosidase activity.

Received 22 November 2001; accepted 10 January 2002.

1. Medzhitov, R. & Janeway, C. A.Jr. Innate immune recognition and control of adaptive immune responses. *Semin. Immunol.* **10,** 351–353 (1998).
2. McCarthy, J. V., Ni, J. & Dixit, V. M. RIP2 is a novel NF-κB-activating and cell death-inducing kinase. *J. Biol. Chem.* **273,** 16968–16975 (1998).
3. Inohara, N., del Peso, L., Koseki, T., Chen, S. & Núñez, G. RICK, a novel protein kinase containing a caspase recruitment domain, interacts with CLARP and regulates CD95-mediated apoptosis. *J. Biol. Chem.* **273,** 12296–12300 (1998); erratum *J. Biol. Chem.* **273,** 18675 (1998).
4. Thome, M. *et al.* Identification of CARDIAK, a RIP-like kinase that associates with caspase-1. *Curr. Biol.* **8,** 885–888 (1998).
5. Yip, H. C. *et al.* Adjuvant-guided type-1 and type-2 immunity: infectious/noninfectious dichotomy defines the class of response. *J. Immunol.* **162,** 3942–3949 (1999).
6. Finkelman, F. D. *et al.* Lymphokine control of *in vivo* immunoglobulin isotype selection. *Annu. Rev. Immunol.* **8,** 303–333 (1990).
7. Mosmann, T. R. & Coffman, R. L. TH1 and TH2 cells: different patterns of lymphokine secretion lead to different functional properties. *Annu. Rev. Immunol.* **7,** 145–173 (1989).
8. Paul, W. E. & Seder, R. A. Lymphocyte responses and cytokines. *Cell* **76,** 241–251 (1994).
9. Yang, J., Murphy, T. L., Ouyang, W. & Murphy, K. M. Induction of interferon-gamma production in Th1 CD4 + T cells: evidence for two distinct pathways for promoter activation. *Eur. J. Immunol.* **29,** 548–555 (1999).
10. Thierfelder, W. E. *et al.* Requirement for Stat4 in interleukin-12-mediated responses of natural killer and T cells. *Nature* **382,** 171–174 (1996).
11. Kaplan, M. H., Sun, Y. L., Hoey, T. & Grusby, M. J. Impaired IL-12 responses and enhanced development of Th2 cells in Stat4-deficient mice. *Nature* **382,** 174–177 (1996).
12. Trinchieri, G. Interleukin-12: a proinflammatory cytokine with immunoregulatory functions that bridge innate resistance and antigen-specific adaptive immunity. *Annu. Rev. Immunol.* **13,** 251–276 (1995).
13. Dai, W. J. *et al.* Impaired macrophage listericidal and cytokine activities are responsible for the rapid death of *Listeria monocytogenes*-infected IFN-γ receptor-deficient mice. *J. Immunol.* **158,** 5297–5304 (1997).
14. DiTirro, J. *et al.* Disruption of the cellular inflammatory response to *Listeria monocytogenes* infection in mice with disruptions in targeted genes. *Infect. Immun.* **66,** 2284–2289 (1998).
15. Inohara, N., Ogura, Y., Chen, F. F., Muto, A. & Nuñez, G. Human Nod1 confers responsiveness to bacterial lipopolysaccharides. *J. Biol. Chem.* **276,** 2551–2554 (2001).
16. Hugot, J. *et al.* Association of NOD2 leucine-rich repeat variants with susceptibility to Crohn's disease. *Nature* **411,** 599–603 (2001).
17. Ogura, Y. *et al.* A frameshift mutation in NOD2 associated with susceptibility to Crohn's disease. *Nature* **411,** 603–606 (2001).
18. Inohara, N. *et al.* An induced proximity model for NF-κB activation in the Nod1/RICK and RIP signaling pathways. *J. Biol. Chem.* **275,** 27823–27831 (2000).
19. Ogura, Y. *et al.* Nod2, a Nod1/Apaf-1 family member that is restricted to monocytes and activates NF-κB. *J. Biol. Chem.* **276,** 4812–4818 (2001).
20. Girardin, S. E. *et al.* CARD4/Nod1 mediates NF-κB and JNK activation by invasive *Shigella flexneri*. *EMBO Rep.* **2,** 736–742 (2001).
21. Reiner, S. L., Zheng, S., Corry, D. B. & Locksley, R. M. Constructing polycompetitor cDNAs for quantitative PCR. *J. Immunol. Methods* **165,** 37–46 (1993); erratum *J. Immunol. Methods* **173,** 133; **175,** 275 (1994).
22. Khan, K. D. *et al.* Induction of the Ly-6A/E gene by interferon alpha/beta and gamma requires a DNA element to which a tyrosine-phosphorylated 91-kDa protein binds. *Proc. Natl Acad. Sci. USA* **90,** 6806–6810 (1993).

Acknowledgements

We thank V. Dixit for human RIP2 cDNA; T. Parks for Nod1 cDNA; T. Roni and S. Smale for CD4-TLR4 cDNA; K. Shaui and X.-F. Qin for reagents and advice; and R. L. Modlin for critical reading of the manuscript. A.I.C. is supported by the Medical Scientist Training Program; P.W.D. is a Lymphoma and Leukemia Society Research Fellow; and G.C. is a Lymphoma and Leukemia Society Research Scholar.

Competing interests statement

The authors declare that they have no competing financial interests.

Correspondence and requests for materials should be addressed to G.C. (e-mail: genhongc@microbio.ucla.edu). The sequence for murine Rip2 cDNA has been deposited in GenBank under accession number AF461040.

RICK/Rip2/CARDIAK mediates signalling for receptors of the innate and adaptive immune systems

Koichi Kobayashi*, Naohiro Inohara†, Lorraine D. Hernandez‡, Jorge E. Galán‡, Gabriel Núñez†, Charles A. Janeway*§, Ruslan Medzhitov*§ & Richard A. Flavell*§

** Section of Immunobiology, and the § Howard Hughes Medical Institute, Yale University School of Medicine, New Haven, Connecticut 06520, USA*
† Department of Pathology and Comprehensive Cancer Center, University of Michigan Medical School, Ann Arbor, Michigan 48109, USA
‡ Section of Microbial Pathogenesis, Boyer Center for Molecular Medicine, Yale School of Medicine, New Haven, Connecticut 06536, USA

The immune system consists of two evolutionarily different but closely related responses, innate immunity and adaptive immunity. Each of these responses has characteristic receptors—Toll-like receptors (TLRs) for innate immunity and antigen-specific receptors for adaptive immunity. Here we show that the caspase recruitment domain (CARD)-containing serine/threonine kinase Rip2 (also known as RICK, CARDIAK, CCK and Ripk2)[1–4] transduces signals from receptors of both immune responses. Rip2 was recruited to TLR2 signalling complexes after ligand stimulation. Moreover, cytokine production in Rip2-deficient cells was reduced on stimulation of TLRs with lipopolysaccharide, peptidoglycan and double-stranded RNA, but not with bacterial DNA, indicating that Rip2 is downstream of TLR2/3/4 but not TLR9. Rip2-deficient cells were also hyporesponsive to signalling through interleukin (IL)-1 and IL-18 receptors, and deficient for signalling through Nod proteins—molecules also implicated in the innate immune response. Furthermore, Rip2-deficient T cells showed severely reduced NF-κB activation, IL-2 production and proliferation on T-cell-receptor (TCR) engagement, and impaired differentiation to T-helper subtype 1 (T_H1) cells, indicating that Rip2 is required for optimal TCR signalling and T-cell differentiation. Rip2 is therefore a signal transducer and integrator of signals for both the innate and adaptive immune systems.

Rip2 is a serine/threonine kinase[1–4] that carries a CARD at its carboxy terminus, and shares sequence similarity with a serine/threonine kinase, Rip, which is essential for NF-κB activation through the tumour-necrosis factor (TNF) receptor[5]. *In vitro* studies have shown that Rip2 can associate with a variety of other CARD-containing molecules through CARD–CARD interactions[1–3]. Moreover, overexpression of Rip2 causes activation of NF-κB and Jun amino-terminal kinase (JNK)[1–4]. NF-κB activation by Rip2 is inhibited by dominant negative TRAF6 (ref. 4), a signalling molecule that is downstream of TLRs. Furthermore, we found that expression of Rip2 was induced in macrophages on stimulation with lipopolysaccharide (LPS) (Fig. 1a, b). These observations led us to consider the possibility that Rip2 is involved in signalling in the innate immune system. To assess the physiological role of Rip2 in signalling in the innate immune system, we generated Rip2-deficient mice by homologous recombination of embryonic stem cells. A gene-targeting construct was generated to replace the two exons coding for murine *Rip2* with a neomycin-resistance gene (*neo*^{r}) (Fig. 1c). Homologous recombination in embryonic stem cells was confirmed by Southern blot analysis (Fig. 1d), and the absence of Rip2 expression in homozygous animals was confirmed by western blot (Fig. 1e). Rip2-deficient mice were born in the expected mendelian ratio, and showed no gross developmental abnormalities and no abnormal composition of lymphocytes as determined by flow cytometry (data not shown).

© 2002 Macmillan Magazines Ltd